Materials Science and Engineering C 31 (2011) 494–498

Contents lists available at ScienceDirect

Materials Science and Engineering C

journal homepage: www.elsevier.com/locate/msec

Short Communication

NaCl doping and the conductivity of agar phantoms

D. Bennett

Department of Electrical & Computer Engineering, The George Washington University, Washington, D.C. 20052, USA

ARTICLE INFO

Article history:
Received 7 June 2010
Received in revised form 5 August 2010
Accepted 13 August 2010
Available online 25 August 2010

Keywords:
Agar
Conductivity measurement
Impedance imaging
Molar conductivity
Phantom

ABSTRACT

A recipe for manipulating the conductivity of agar impedance-imaging phantoms through their NaCl (salt) content is reexamined. The conductivities at frequencies 100 kHz and below are characterized for phantoms created with the recipe. The data are compared against the recipe's predictive formula for conductivity as a function of salt content. Based on analysis of the data a modified version of the conductivity formula is generated. The modified predictive formula better approximates the observed NaCl dependence of conductivity in phantoms with salt concentrations under 0.1 M. The experimental data also provide verification for the asymptotic dependence of contact impedance on frequency and phantom conductivity. The results of these experiments will be helpful in better constructing agar phantoms to electrical specifications for future impedance-imaging experiments.

1. Introduction

Agar phantoms provide a useful way of testing bio-impedance-imaging systems. These phantoms can be physically molded and their electrical properties altered to mimic a variety of tissue types and anatomical configurations. The conductivities of my phantoms, which are based on a recipe from [12], are controlled by the concentration of NaCl used in their preparation. The approximate relationship between the salt concentration and the agar's conductivity σ is given by [12][1]:

$$\left(\sigma, {}^{S}/_{m}\right) = \begin{cases} 200\left({}^{S\cdot mL}/_{m\cdot g}\right) \times \dfrac{(grams\ of\ NaCl)}{(solution\ volume,\ mL)} \\ or \\ 11.69\left({}^{S\cdot L}/_{m\cdot mol}\right) \times \dfrac{(moles\ of\ NaCl)}{(solution\ volume,\ L)} \end{cases}. \quad (1)$$

However, experiments with these phantoms have shown slightly higher than expected conductance values. Therefore, a series of experiments was performed to verify the salt concentration dependence of the agar's conductivity set forth in Eq. (1).

Six agar phantoms were made by combining a molten agar solution with saline solutions of various concentrations. Samples from each phantom were taken and their conductivities were determined for several frequencies: 67, 100, and 500 Hz; and 1, 5, 10, 50, and 100 kHz. A functional relationship between the phantoms' salt concentrations and their conductivities was estimated based on the gathered data. Finally, this relationship was compared with Eq. (1).

2. Background

The concentration dependence of a solution's conductivity is defined by the molar conductivity. In simplest terms it is the ratio of a solution's conductivity to its concentration. The coefficient $11.69 S*L/(m*mol)$ in Eq. (1) is a prime example. In this case, it relates the solution concentration of NaCl to the observed agar conductivity. In general, molar conductivity varies with concentration and the choice of solvent. For a strong electrolyte like NaCl (in water), molar conductivity declines slightly with increasing concentration. For very dilute solutions the molar conductivity of a strong electrolyte is described by Kohlrausch's Law [1]: $G = G_0 - K*c^{1/2}$, where G_0 is the low-concentration limit of molar conductivity ($G_0 = \lim G, c \to 0^+$), K is the Kohlrausch constant, and c is concentration.

Since agar gels, like the ones used in the phantoms discussed here, consist of small amounts of agar dispersed in an aqueous phase, their conductive properties should be dominated by those of their aqueous component. Interestingly enough, the molar conductivity value in Eq. (1) is close to the limiting molar conductivity of NaCl in water, at room temperature, $12.64 S*L/(m*mol)$ [1].

3. Materials and methods

3.1. Preparation of phantoms

First, a primary saline solution was created by mixing enough deionized water with NaCl to produce around 40 mL of 0.136 M NaCl solution. Four more saline solutions were created according to the

E-mail address: dbennett@gwu.edu.

[1] Note: The relationship in [13] is expressed in terms of solvent volume rather than solution volume, but for the low solution concentrations presented in this work the two quantities are approximately equivalent. Solution volume was a more convenient measure to use for the dilutions described in Section 3.1.

0928-4931/$ – see front matter © 2010 Elsevier B.V. All rights reserved.
doi:10.1016/j.msec.2010.08.018

Table 1
Dilution table showing the quantities used to prepare the saline solutions. The last column shows the saline concentration of the agar phantom prepared with the corresponding saline solution. All concentrations are given in terms of grams of solute per milliliter of solution.

Solution #	NaCl solution (mL)	H_2O (mL)	NaCl concentration (g/mL)	Agar–saline NaCl conc. (g/mL)
1	40.5	0	7.96E−03	3.90E−03
2	20.3 (of #1)	19.6	4.05E−03	1.99E−03
3	20.2 (of #2)	20.4	2.01E−03	9.88E−04
4	19.8 (of #3)	20.7	9.85E−04	4.83E−04
5	20.0 (of #4)	19.5	4.99E−04	2.45E−04
6 (no NaCl)	0	13	0	0

dilution table (Table 1) below: for example, Solution #2 was made by diluting 20.3 mL of Solution #1 with 19.6 mL of deionized water. Once all five solutions were prepared, 13 mL of each solution was added to separate vials that would become the molds for the phantoms. To a sixth vial, 13 mL of plain deionized water was added.

Approximately 3 g of high gel strength, powdered agar (Sigma-Aldrich, USA) was thoroughly dissolved in boiling deionized water to create 100 mL of molten agar solution. The hot agar solution was carefully added in 13.5 mL aliquots to the 13 mL of saline solution in each of the phantom molds. The agar mixtures were well stirred and then allowed to cool to room temperature and gel.

3.2. Determining conductivity

The electrical properties of the agar were characterized using the circuitry shown in Fig. 1. The sample chamber in the figure has a pair of flat, circular, solder coated electrodes at either end to apply a potential to a cylindrical section removed from the phantoms. The source potential in the test circuitry, V_{ac}, is a sinusoid supplied by a Wavetek 182A function generator. Voltage measurements across the sample chamber and a 4.7 kΩ resistor (R_s in Fig. 1) are made with a Tektronix TDS 210 digital oscilloscope. The current through a phantom sample is determined by calculating the ratio of the voltage drop across R_s and resistance of R_s. The current magnitude is also monitored through a Tektronix DMM912 multimeter (shown as the amp meter in Fig. 1) for immediate readout.

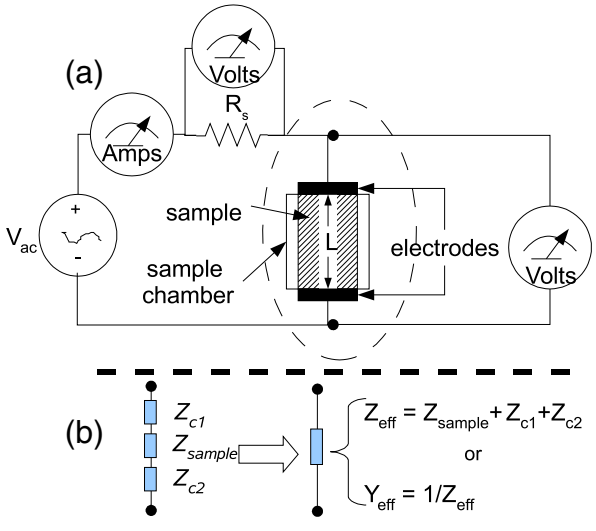

Fig. 1. (a) Depiction of circuitry for measuring the effective admittance (Y_{eff} = (*Amps*)/(*Volts*)) of agar samples with length L; (b) equivalent circuit model of encircled region in (a) showing the measured Y_{eff}'s dependence on both a sample's impedance, Z_{sample}, and electrode-sample contact impedances, Z_{c1} and Z_{c2}.

For each phantom, samples of various lengths were tested. Using the current/voltage measurements the effective admittances ($Y_{eff} = I/V$, where I and V are the phasor representations of the sample current and voltage, respectively; see the equivalent circuit model in Fig. 1) were calculated for the samples at the following frequencies: 67; 100; 500; 1000; 5000; 10,000; 50,000; and 100,000 Hz. All measurements were carried out at room temperature.

Each phantom's collection of admittance values at a given frequency f is approximately related to the tested sample's length L by the model in Eq. (2), which is derived from Ohm's Law. With the help of the nonlinear least-squares fitting routine in [8], the admittances were regressed on their corresponding lengths according to this model (see Fig. 2 for an example). Finally, conductivity was estimated from the regression parameter P_1 through the relationship $\sigma = \text{real}(P_1/(\text{electrode area}))$. Plots of conductivity vs. frequency are shown in Fig. 3 for all six phantoms.

$$Y_{eff}(f) = \frac{P_1(f)}{L + P_2(f)} + N\left(0, s^2\right) \tag{2}$$

Where $P_1 = (\sigma + j2\pi f\varepsilon) * (\text{electrode area})$, $P_2 = (Z_{c1} + Z_{c2}) * P_1$, the Z_c's are electrode contact impedances (see Fig. 1-b), ε is the sample's permittivity, and $N(0,s^2)$ is a Gaussian random variable with zero mean and standard deviation s.

3.3. Conductivity and NaCl concentration

Linear regression analysis was used to find the dependence of conductivity on saline concentration (3a). The regression parameters were computed for the conductivities aggregated over all frequencies as well as for each frequency separately so that any frequency dependence could be identified (see Table 2). Due to differences in the variances associated with the conductivity estimates (i.e., heteroskedasticity), weighted least squares (WLS) was employed to find the parameters m and b in Eq. (3a). The WLS estimation problem is summarized by Eq. (3b) (notice the inverse of the conductivities' standard deviations $s(c_i,f_j)$ are used as the weights). The equations of the WLS estimators for m and b are given in Eqs. (3c) and (3d), respectively (see [7] for a discussion of the WLS estimator and linear analysis of heteroskedastic data).

$$\sigma\left(c_i, f_j\right) = m \cdot c_i + b + N\left(0, s^2\left(c_i, f_j\right)\right) \tag{3a}$$

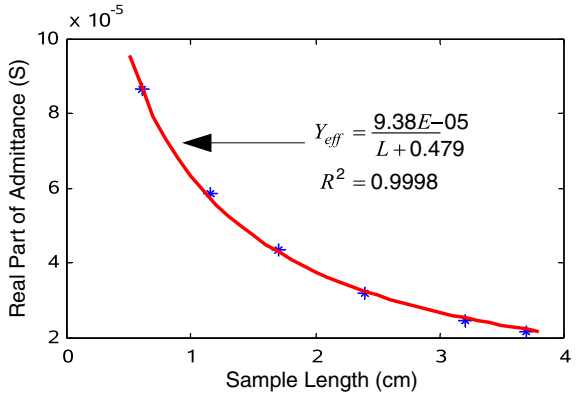

Fig. 2. Phantom #6's (see Table 1) collection of effective admittances (the * points) plotted against the lengths of the samples measured at 67 Hz. The regression curve for the data (solid line), based on the model in Eq. (2), is also shown.

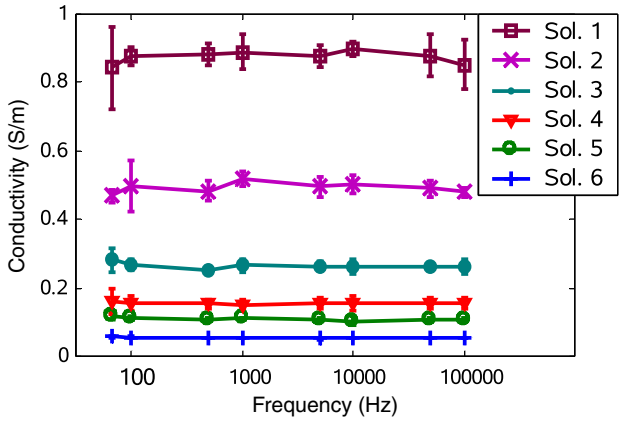

Fig. 3. Graph of conductivity vs. frequency for phantoms with various salt concentrations; error bars indicate 95% confidence intervals.

where

$$(m,b) = \arg\min_{(m,b)} \left(\sum_{i \text{ or } (i,j)} \left(\frac{\sigma(c_i,f_j) - (m \cdot c_i + b)}{s(c_i,f_j)} \right)^2 \right) \tag{3b}$$

$$m = \frac{\sum \frac{1}{s^2(c_i,f_j)} \sum \frac{\sigma(c_i,f_j)\cdot c_i}{s^2(c_i,f_j)} - \sum \frac{\sigma(c_i,f_j)}{s^2(c_i,f_j)} \sum \frac{c_i}{s^2(c_i,f_j)}}{\sum \frac{1}{s^2(c_i,f_j)} \sum \frac{c_i^2}{s^2(c_i,f_j)} - \left(\sum \frac{c_i}{s^2(c_i,f_j)} \right)^2} \tag{3c}$$

$$b = \frac{\sum \frac{\sigma(c_i,f_j)\cdot c_i}{s^2(c_i,f_j)} - m \cdot \sum \frac{c_i}{s^2(c_i,f_j)}}{\sum \frac{1}{s^2(c_i,f_j)}} \tag{3d}$$

$\sigma(c_i,f_j)$ is the conductivity at frequency f_j for a saline concentration of c_i, $s(c_i,f_j)$ is the estimate of this conductivity's standard deviation, m and b are the slope and y-intercept regression parameters, respectively, and the summations (Σ) are taken over i for the f dependent regression parameters and over (i,j) for the f independent parameters.

4. Results and discussion

The experiments and results presented in this paper examined the conductivity of colloidal agar impedance phantoms as a function of frequency and NaCl content. The frequency responses shown in Fig. 3 reveal that the conductivity of each phantom is constant to within 4% of its respective mean over the range of frequencies from 67 Hz to 100 kHz. Another important observation is that the effect of NaCl concentration on conductivity of the phantoms is approximately linear, as evidenced by the high R^2 values in Table 2 and the conductivity vs. concentration plot in Fig. 4. Taken together these two observations – the approximately constant frequency responses and the strong linear association of conductivity and salt concentration – imply that a frequency-independent, linear model well approximates the salt concentration dependence of the conductivity data:

$$\left(\sigma,^{S}/_{m}\right) = 215 \times \frac{(grams\ of\ NaCl)}{(solution\ volume,\ mL)} + 0.0529. \tag{4}$$

The above expression is plotted in Fig. 4 along with the line from Eq. (1). A crucial difference between the two lines is their y-intercepts. Clearly the y-intercept of Eq. (1) is zero, but for the regression line in Eq. (4) it is 0.0529 S/m. To verify that this y-intercept (or offset) was not the result of a simple experimental error, such as contaminated deionized water, three additional tests were performed according to the methodology described in Section 3.2.

The first test examined the deionized water in order to make sure that it was not tainted. The second test was to check the reproducibility of the offset by measuring an additional agar phantom produced separately from the original set that was tested. The third characterized a slurry of powdered agar and deionized water to see if the offset could possibly be attributed to a water soluble contaminant in the agar (e.g., NaCl). The conductivity of the deionized water was too low (less than 0.2 mS/m) to reliably measure; consequently, it is not the source of the offset. Measurements of the additional phantom (produced with no added NaCl) found its conductivity was 0.0544 S/m. This is consistent to within 5% of the offset in Eq. (4) proving it is reproducible. The slurry, created by mixing 0.09 g of agar with 10 mL of room temperature deionized water, displayed a conductivity of 0.0073 S/m. This last result implies that most of the observed offset's magnitude is due to a component of the agar phantoms that is not soluble at room temperature. Taken together these three results suggest that there is a link between the agar and the offset. More extensive testing would have to be done to determine how it is affected by the type and amounts of agar used in the phantoms.

Further evidence of the non-zero y-intercept can be found in the results in [3], [5], and [9]. Notably, the offset in Eq. (4) is similar to the 0.059 S/m offset found in [5], which looked at the effect of NaN3 and PVC doping on phantoms with higher agar content than those studied here.

Aside from the y-intercepts, there is also a discrepancy between the slopes of Eqs. (4) (215S*mL/m/g) and (1) (200S*mL/m/g). The disagreement is small, however, validating the equation from [12] as a way of estimating the *change* in agar's conductivity with the addition of NaCl.

Table 2
Table of regression parameters for conductivity as a function of salt concentration. The Δ columns define 95% confidence intervals for the associated parameters P, i.e., the intervals range from $P-\Delta$ to $P+\Delta$.

Frequency (Hz)	Slope ($S*mL/(m*g)$)	Δ Slope	y-Intercept (S/m)	Δ Intercept	R^2
67	209.5	14.3	0.0574	0.0053	1.00
100	213.8	12.3	0.0557	0.0038	1.00
500	209.1	10.6	0.0524	0.0020	1.00
1000	224.7	15.5	0.0525	0.0022	1.00
5000	214.3	5.9	0.0521	0.0014	1.00
10,000	217.6	5.0	0.0530	0.0009	1.00
50,000	215.7	5.3	0.0527	0.0013	1.00
100,000	213.5	4.4	0.0533	0.0010	1.00
All freqs.	214.8	2.8	0.0529	0.0006	1.00

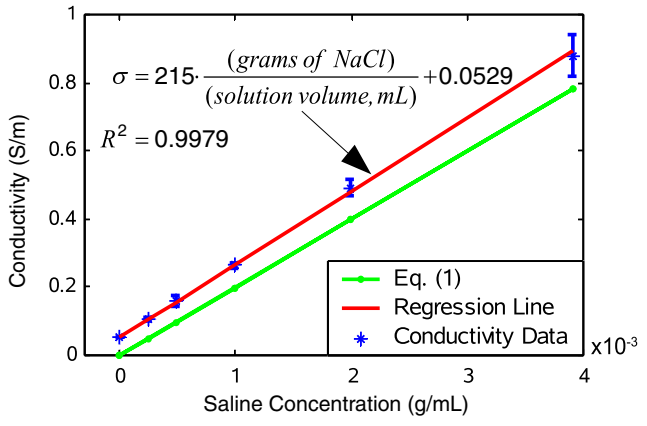

Fig. 4. Graph of estimated conductivity at 50 kHz (* points) vs. salt concentration (error bars indicate 95% confidence intervals). Additionally, the regression line from Eq. (4) (solid line) and predicted conductivity from Eq. (1) (dotted line) are presented for comparison.

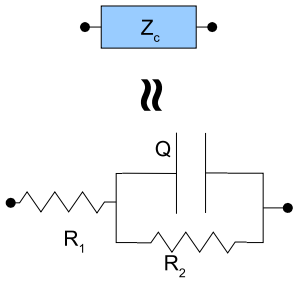

Fig. 5. Diagram of equivalent circuit frequently used to approximate contact impedance Z_c. The R's represent resistors and Q is a capacitor.

Nevertheless, for the preparation of low-conductivity, agar phantoms, failure to account for an offset like the one in Eq. (4) can lead to significantly different conductivity values than expected. For example, a phantom to replicate lung tissue (inflated) at 100 kHz should have a conductivity of about 0.08 S/m [2], but if it is manufactured using Eq. (1), the actual conductivity, according to Eq. (4), would be closer to 0.14 S/m; this is a 75% difference. Clearly, this would have implications for impedance-imaging systems using the phantom for realistic imaging studies, calibration, or safety testing.

Acknowledgements

The author acknowledges financial support by the National Science Foundation and the Susan G. Komen Breast Cancer Foundation. I thank the Chemistry Department of The George Washington University for procuring some of the materials needed for the experiments. I would also like to express my appreciation to my faculty advisor Prof. M. H. Loew of the Electrical & Computer Engineering Department for his thoughtful and constructive criticism of this composition and its related works.

Appendix A. The unwanted parameter: contact impedance

In addition to finding the conductivity the measurements gathered provide insight into the saline concentration and frequency dependence of contact impedance. Contact impedance, Z_c, (or specific contact impedance,[2] z_c) is a parasitic (i.e., undesirable) parameter used to model the variable impedance layer that forms at the interface between an electrode and the material it has contact with. Its magnitude tends to decline with frequency [6, p. 195] [11]. It's often modeled by a simple resistor–capacitor circuit like the one shown in Fig. 5, where the resistive (R) and capacitive (Q) components are in general functions of frequency and current [6, p. 194]. The material properties of the electrode and the substance in contact with the electrode also affect the magnitude of contact impedance: [10] and [4] report an inverse relationship between specific contact impedance, z_c, and conductivity, σ.

The z_c for the electrode–agar interfaces in the conductivity experiment (Section 3.2) can therefore be approximated by a model synthesized from the observations in [4] and the circuit impedance for

[2] There is often ambiguity in the literature over the usage of the term "contact impedance." Sometimes it is used to refer to a lumped impedance parameter that depends on electrode surface area and has units of Ω. This quantity is simply referred to here as "contact impedance" or Z_c. The other usage of the term "contact impedance" refers to a parameter that is independent of electrode surface area and that has units of Ωm^2. For distinction I've referred to this form of contact impedance, z_c, as "specific contact impedance." The approximate relationship between the two contact impedances is $Z_c \approx z_c/(\text{electrode area})$.

Table 3
Regression coefficients for Eqs. (6) and (7) used to describe z_c.

R_1 parameters		R_2 parameters		$R_2{*}Q$
q_1 (Ωm^2)	q_2 (m)	s_1 (Ωm^2)	s_2 (m)	k (s/radian)
0.0017	0	34.15	1.57	3.67

Fig. 5. Eq. (5) designates a relationship between z_c and σ similar to that from [4]:

$$z_c(f,c) = b_1(f) + \frac{b_2(f)}{\sigma(c) + j2\pi f\varepsilon(c)} \approx b_1(f) + \frac{b_2(f)}{215c + 0.0529}. \quad (5)$$

Taking advantage of Eq. (4) in conjunction with the observation that $\sigma \gg j2\pi f\varepsilon$ for the phantoms helps simplify Eq. (5) and makes explicit the c (in g/mL) dependence. Note, that although we can safely ignore the imaginary $j2\pi f\varepsilon$ term, $b_1(f)$ and $b_2(f)$ are in general complex valued functions, independent of c. In order to reconcile Eq. (5) for z_c with the impedance of the circuit model in Fig. 5 (see Eq. (6)), one can substitute into Eq. (6) the formulas in Eq. (7), which were inspired in form by Eq. (5). The q, s, and k model parameters in Eq. (7) stand for constants that can be determined from experimental observations.

$$z_c(f,c) = R_1(f,c) + \frac{R_2(f,c)}{1 + j2\pi f R_2(f,c)Q(f,c)} \quad (6)$$

$$R_1 = q_1 + \frac{q_2}{\sigma},\ R_2 = s_1 + \frac{s_2}{\sigma},\ Q = \frac{k}{R_2} \quad (7)$$

Approximating z_c for the agar–electrode interface is done in much the same way as finding the agar's conductivity (Section 3.2). Samples from one of the agar gels described in Section 3.1 are measured with the testing setup depicted in Fig. 1. The samples are cut to have several different lengths L. The admittances of these samples, Y_{eff}, are calculated from the currents and voltages measured at frequencies from 67 Hz to 100 kHz. The measured admittances are related to L by the model in Eq. (2). By using the nonlinear fitting tools in [8] to estimate the model parameters P_1 and P_2 from Eq. (2), we can approximate the specific contact impedance z_c with the formula:

$$z_c = (\text{electrode area}) \cdot \frac{P_2}{2P_1}. \quad (8)$$

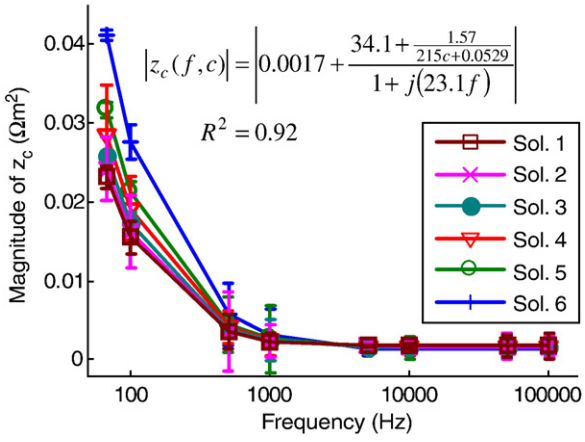

Fig. 6. Graph of specific contact impedance, z_c, vs. frequency, f, for phantoms with various salt concentrations; error bars indicate the maximum observed deviation by z_c computed with the measurement data (see Eq. (8)) from the model delineated in Eqs. (6) and (7) (solid lines).

This procedure was followed for all six phantoms described in Section 3.1 to obtain z_c estimates for six different agar conductivities (and correspondingly their saline concentrations c).

The q, s, and k constants from Eq. (7) were computed for the set of z_c's by fitting them to Eqs. (6) and (7) through a nonlinear least-squares procedure [8] (see Table 3 for coefficient values). Fig. 6 shows the magnitude of the fitted curve as a function of frequency for the various salt concentrations of the phantoms. As predicted by the model in Eqs. (6) and (7) the observed z_c's Eq. (8) decline asymptotically with increasing frequency and NaCl concentration. Overall there is good agreement between the observed z_c's and the model predictions ($R^2 = 0.92$ and the standard deviation of the prediction error is $0.0023\Omega m^2$).

References

[1] Peter Atkins, Molecules in motion, Physical Chemistry, 6th ed, W.H. Freeman & Company, New York, 1998, p. 737.
[2] S. Gabriel, R.W. Lau, C. Gabriel, Physics in Medicine and Biology 41 (1996) 2257.
[3] S. Nahum Goldberg, Muneeb Ahmed, G. Scott Gazelle, Jonathan B. Kruskal, Juan Carlos Huertas, Elkan F. Halpern, Brian S. Oliver, Robert E. Lenkinski, Radiology 219 (2001) 160.
[4] Jin-Ha Hwang, K.S. Kirkpatrick, T.O. Mason, E.J. Garboczi, Solid State Ionics 98 (1997) 94.
[5] Hirokazu Kato, Tetsuya Ishida, Physics in Medicine and Biology 32 (1987) 222.
[6] Michael Neuman, Biopotential electrodes, in: John G. Webster (Ed.), Medical Instrumentation — Application and Design, John Wiley & Sons, Inc., New York, 1998.
[7] G.S. Maddala, Heteroskedasticity, Introduction to Econometrics, 2nd ed, Prentice Hall, Inc, Englewood Cliffs, 1992, p. 209.
[8] Matlab Version 5.3, The Mathworks, Inc, Natick, 1999.
[9] Tong In Oh, Hwan Koo, Kyung Heon Lee, Sang Min Kim, Jeehyun Lee, Sung Wan Kim, Jin Keun Seo, Eung Je Woo, Physiological Measurement 29 (2008) 295.
[10] Kevin Paulson, William Breckon, Michael Pidcock, SIAM Journal on Applied Mathematics 52 (1991) 1014.
[11] M.R. Stoneman, M. Kosempa, W.D. Gregory, C.W. Gregory, J.J. Marx, W. Mikkelson, J. Tjoe, V. Raicu, Physics in Medicine and Biology 52 (2007) 6592.
[12] T. Yorkey, *Comparing Reconstruction Methods for Electrical Impedance Tomography*, PhD Thesis, University of Wisconsin, 1986.